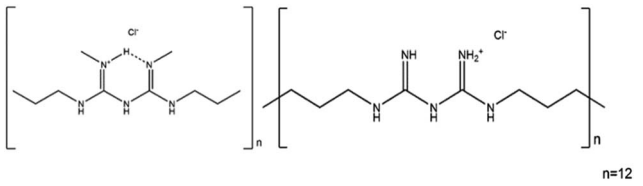

Fig. 1 Schematic structure of mono-protonated PHMB with chloride as a counter ion.

reasonable cost.[8] This polymer has an average molecular weight of 2648 ± 50 g mol^{-1} and an average of 10–13 repeating units per chain (Fig. 1).[12] Bacterial resistance is very unlikely to occur due to non-specific and multi-target PHMB antibacterial action,[8,12] acting as a bacteriostatic if administered at low concentrations (1–10 μg mL^{-1}) and as a bactericidal at high doses (>10 μg mL^{-1}).[13]

The majority of PHMB applications has been carried out in "free form"[7 10] but this is far from appropriate for applications in the environment, where residual traces of PHMB would certainly not be acceptable. An inherent disadvantage of PHMB is the high solubility in water,[8] which makes its removal from the environment extremely difficult. The immobilization of PHMB in insoluble supports can be an interesting approach to inactivate pathogenic microorganisms, preventing any risk of environmental contamination. Additionally, when stable chemicals like PHMB[9] are immobilized on solid supports, they can be easily removed, recovered and reused, which makes this a less expensive technology.

In this work we attempted the encapsulation of commercially available PHMB (VANTOCIL® IB) in silica capsules with porous shells *via* a water-in-oil microemulsion, through a single (one-step) polymerization step process. There are reports of PHMB functionalization onto cationic silver nanoparticles[13] but, to the best of our knowledge, the immobilization/encapsulation of this antimicrobial agent in inorganic silica capsules is a new topic and has not been reported yet.

The synthesis and characterization of silica particles encapsulating PHMB was performed by different techniques and the antibacterial activity of the capsules was evaluated as a starting ground for future applications such as surface cleansers or coatings.

2. Experimental section

2.1. Materials

Ammonia solution 25–28% (NH_4OH), Span® 85, Tween® 20, tetraethyl orthosilicate 99.9% (TEOS) and PBS (Phosphate Buffer Solution) were purchased from Sigma-Aldrich. Poly(hexamethylene biguanide) hydrochloride (PHMB) was supplied as a 20% w/w solution in water (Arch UK Biocides) and cyclohexane was obtained from Merck. Ethanol was provided by Carlo Erba reagents, sodium phosphate dibasic and sodium phosphate monobasic were supplied by Riedel-de Häen. All reagents were of analytical grade and used without any further purification.

2.2. Synthesis of silica capsules loaded with PHMB (PHMB@silica capsules)

Silica capsules were prepared through a reverse emulsion, using Span® 85 and Tween® 20 as surfactants, cyclohexane as continuous phase and an ammonia solution as catalyst.[6] An oil phase was prepared by dissolving 1 g of Span® 85 in 50 mL of cyclohexane. Then, one drop of Tween® 20 in 5 mL of PHMB solution, followed by the addition of 2.0 mL of ammonia solution (25–28%) (water phase), were added to the oil phase under stirring and a water-in-oil microemulsion was obtained. After a few minutes stirring, 2.0 mL of TEOS was added to the w/o microemulsion under vigorous stirring and kept in a closed vessel for 24 h. The precipitate was then filtered, washed with cyclohexane and dried at 60 °C. A small portion of these capsules was calcined at 550 °C, with a heat integrate of 5 °C min^{-1}, in order to determine the content of loaded PHMB. Empty silica capsules were produced by performing the same experimental method but instead of PHMB aqueous solution, the same volume of deionized water was used.

2.3. Capsule characterization

Particle morphology was characterized by scanning electron microscopy (SEM) (Hitachi S-4100 system with electron beam energy of 25 keV).

FTIR analyses of empty silica capsules, PHMB@silica capsules and PHMB were carried out on a Bruker Tensor 27 Spectrometer coupled with an ATR device. PHMB loading into silica capsules was evaluated on a Thermo Scientific Evolution 220 UV-Visible Spectrophotometer.

A Malvern Instruments, NanoSeries Nano ZS, was used to perform dynamic light scattering (DLS) and zeta potential measurements (content of silica capsules in suspension of 0.03 w/v%).

Thermogravimetric analysis (TG/DTA) was carried out in a Sataram Labsys system under air atmosphere, with a heating rate of 10 °C min^{-1} in the temperature range of 20–800 °C.

Nitrogen adsorption–desorption isotherms at 196 °C were acquired on a Micromeritics Gemini 2370 equipment operating in an automatic mode. Samples were previously degassed for 6 h at 150 °C. The specific area (S_{BET}) was calculated by the Brunauer–Emmett–Teller (BET) method and the total pore volume from the total volume of N_2 adsorbed at high relative pressures ($p/p_0 \sim 0.98$).[11] The pore size distribution was analyzed by using the Barrett–Joyner–Halenda (BJH) method.[14]

2.4. Release studies of PHMB from silica capsules

The total release of PHMB from silica capsules (determination of loading content), in different solvents, was monitored by UV-Vis spectrophotometry using a Thermo Scientific Evolution 220 UV-Vis Spectrophotometer. Calibration curves were performed and their correlation coefficient, from at least 5 standards, was higher than 0.9999. A suspension of capsules loaded with PHMB (20 mg) was prepared in 20 mL of solvent (water; PBS pH 7.0; 70% (v/v) ethanol) and kept for 24 h under continuous stirring. At 24 h, aliquots were extracted with a syringe and

filtered through PTFE membrane filters (0.45 μm pore size) to remove capsules. Dilutions were performed when needed. Additionally, at different time periods (0–24 h), a series of aliquots were taken from a capsules suspension (50 mg capsules in 50 mL of solvent) with a syringe and filtered through PTFE membrane filters (0.45 μm pore size) to remove capsules. This study was only performed in PBS at pH 7.4 to establish a direct comparison between PHMB release and antimicrobial assessment results. The maximum release of PHMB was monitored, for both studies, and its concentration and corresponding loading content were determined by UV-Vis spectrophotometry at specific wavelengths.

Encapsulation efficiency was determined according to the following eqn (1)

$$\%\ \mathrm{EE} = n\mathrm{PHMB}_{\mathrm{ext}}/n\mathrm{PHMB}_{\mathrm{i}} \times 100 \quad (1)$$

where $n\mathrm{PHMB}_{\mathrm{ext}}$ is the amount of PHMB extracted from the silica capsules and $n\mathrm{PHMB}_{\mathrm{i}}$ is the initial amount of PHMB used in the encapsulation.

2.5. Assessment of the antimicrobial effect of PHMB silica capsules

The antimicrobial effect of PHMB in silica capsules and PHMB in free form was evaluated using a recombinant bioluminescent strain of *Escherichia coli*.[15] Bacterial cells suspensions (10^7 UFC mL^{-1}) in PBS were exposed to the capsules, for 4 h. The tested concentrations of PHMB@silica capsules were those equivalent to 20 ppm PHMB, which is the minimum inhibitory concentration (MIC) of this biocide against *E. coli*,[16] and a ten-fold higher concentration (200 ppm PHMB). A negative control corresponding to cell suspensions in PBS without any amendment and controls corresponding to equivalent concentrations of empty silica capsules and the surfactants Tween® 20 and Span® 85 used in the preparation of capsules were included. The inactivation was assessed, in real time, as the decrease in bacterial light emission, read in a luminometer (TD-20/20, Turner Designs).

3. Results and discussion

3.1. Synthesis of PHMB@silica capsules

Silica capsules were produced through a water-in-oil emulsion (reverse emulsion) polymerization using Span® 85 and Tween® 20 as surfactants and cyclohexane as continuous phase (Fig. 2). For both empty silica capsules and silica capsules loaded with PHMB (PHMB@silica capsules) white particles were obtained *via* polymerization of silica precursor TEOS.

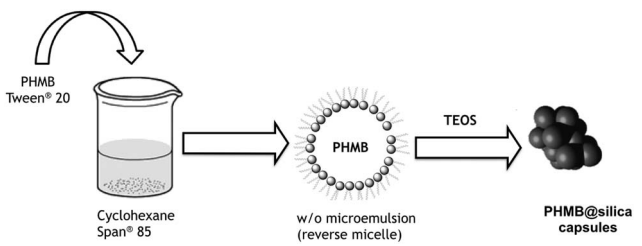

Fig. 2 Synthesis of silica capsules and encapsulation of PHMB.

3.2. Capsules characterization

3.2.1. Scanning electron microscopy. Scanning Electron Microscopy (SEM) was used to analyze the size and shape (morphology) of the synthesized capsules (Fig. 3). The observed particles display a spherical and regular shape, with diameters between 100 and 300 nm for empty capsules and between 270 nm and 1 μm for PHMB@silica capsules. From SEM analysis it is also possible to observe the presence of residual polymer that may have contributed to some degree of aggregation. Comparing both capsules, it is clear that encapsulation of PHMB leads to considerable changes in terms of particle size since a broader distribution of sizes for the loaded material has been observed.

Furthermore, scanning transmission electron microscopy (STEM) analysis confirmed the spherical morphology of PHMB@silica capsules, as observed previously by SEM, and evidenced silica capsules with a wall thickness of approximately of 45 nm and a porous core (Fig. 4).

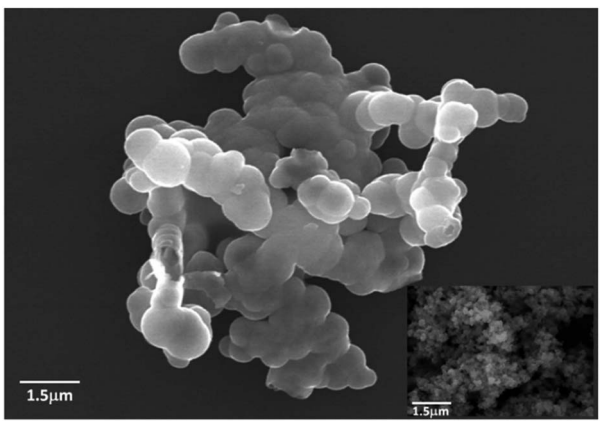

Fig. 3 SEM pictures PHMB@silica capsules (inset empty silica capsules).

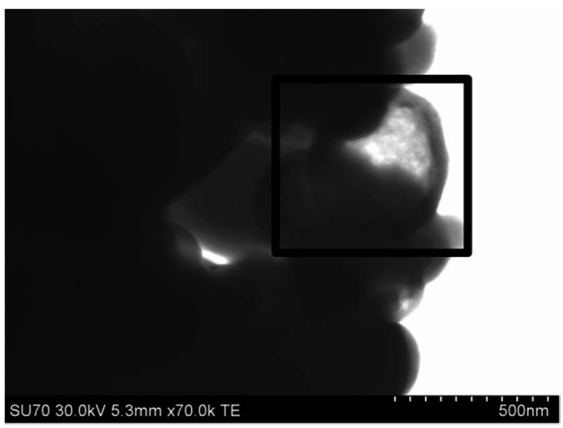

Fig. 4 STEM picture of PHMB@silica capsules.

3.2.2. Zeta potential and particle size analysis. Zeta potential and particle size distribution of synthesized silica capsules have been assessed. According to zeta potential analysis, empty silica capsules have an average zeta potential of *ca.* 28 mV, which is in agreement with the charge associated with SiO_2 functional groups.[17] On the other hand, PHMB@silica capsules have an average zeta potential of *ca.* +60 mV, probably due to the fact that PHMB is a cationic polymer and its presence at the capsule interface determines the positive charge. Noteworthy, the water-in-oil emulsions of PHMB also possess the same average zeta potential.

Regarding the size distributions of synthesized capsules, determined by dynamic light scattering (Fig. 5), empty silica capsules present a narrower distribution of sizes than PHMB-loaded capsules, with peaks ranging from ~100 nm to slightly larger diameters (~300 nm), while for PHMB silica capsules particle size distribution exhibits a peak centered at 164 nm but the presence of larger particles (up to 1.5 μm) leads to a higher average size. The results are consistent with SEM images presented in Fig. 3.

From the results obtained in Section 3.2.1 and 3.2.2, it is clear that PHMB causes significant changes in the particle size. Considering that at least a fraction of PHMB is situated at the interface of the emulsion, this polymer seems to play a role on the way TEOS polymerizes and eventually on how mass transfer between the two phases occur.

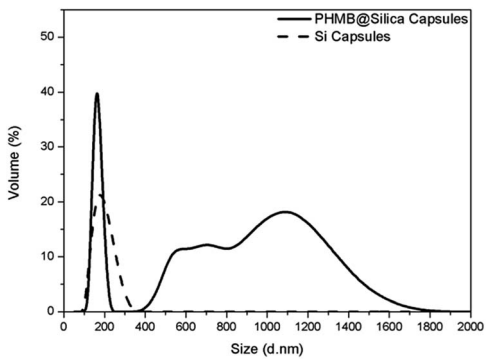

Fig. 5 Size distribution of empty silica capsules and those filled with PHMB.

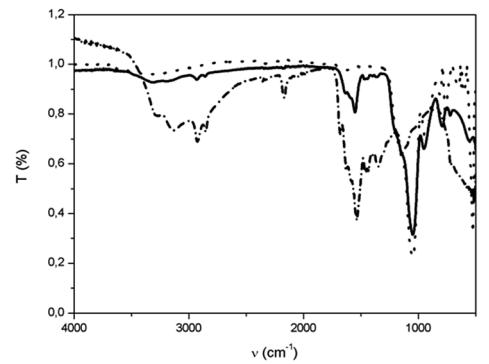

Fig. 6 FTIR spectra of (▬ ● ▬ ● ▬) PHMB (dry), (●●●) empty silica capsules and (▬) PHMB@silica capsules.

3.2.3. FTIR characterization. FTIR analysis of the synthesized capsules was performed to confirm the encapsulation of PHMB. In the FTIR spectra presented in Fig. 6, characteristic bands associated with empty silica capsules can be observed, namely Si–O–Si stretching (1049 cm^{-1}), Si–OH stretching (935 cm^{-1}) and Si–O–Si bending (814 cm^{-1}). Regarding PHMB, N–H stretching can be observed at 3291 and 3157 cm^{-1}, a weak C=N band at 2164 cm^{-1}, as well as characteristic NH_2^+ bending at 1536 cm^{-1}. The presence of PHMB in silica capsules is confirmed by the appearance of peaks that are present in the spectrum of dried PHMB and absent from the FTIR spectra of empty silica capsules. These peaks are visible at 1632 and 1551 cm^{-1} (N–H bending vibrations from imine groups), 1466 and 1366 cm^{-1} (CH_2 bending from alkanes) and 2932 and 2858 cm^{-1} (CH_2 stretching from alkanes), in agreement with data reported in the literature for PHMB.[13,18]

3.2.4. Nitrogen sorption isotherms and pore size distribution. The textural properties of silica capsules (empty and PHMB@silica capsules) were evaluated through adsorption–desorption N_2 isotherms at 196 °C, and are presented in Fig. 7A. The results showed typical multilayer adsorption behavior with different pore size distributions. The main results on silica capsules characterization including specific area (S_{BET}) and total pore volume (V_{total}) are summarised in Table 1. The samples revealed significantly different BET areas, 308 $m^2\ g^{-1}$ and 55 $m^2\ g^{-1}$ for empty and PHMB@silica capsules, respectively, implying that PHMB promotes meaningful changes in the capsules surface area. Furthermore, the pore volume was reduced significantly after PHMB loading, indicating that most pores in the capsules are filled with the antimicrobial agent.[20]

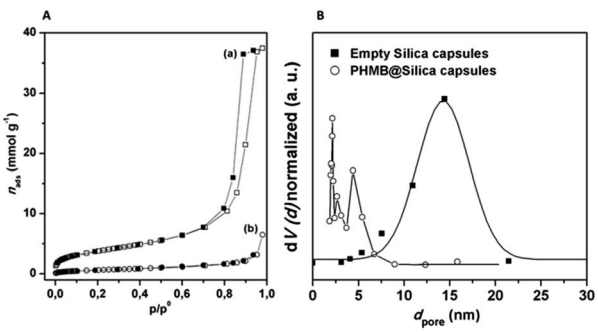

Fig. 7 (A) Nitrogen adsorption desorption isotherms for silica capsules: (a) empty and (b) PHMB@silica capsules open points for adsorption and closed points for desorption and solid line only used for visual guidance. (B) Normalized pore size distribution of Si-based capsules.

Table 1 Surface properties for empty and PHMB-loaded silica capsules as revealed from N_2 adsorption desorption isotherms

Material	S_{BET} ($m^2\ g^{-1}$)	V_{total} ($cm^3\ g^{-1}$)
Silica capsules	308	1.3
PHMB@silica capsules	55	0.22

The N_2 isotherms obtained for empty capsules showed characteristic hysteresis loops, that occur when adsorption–desorption curves do not coincide and are generally associated with capillary condensation taking place in mesoporous materials. For empty silica capsules the hysteresis observed is a type H1, typically characterized by a very well defined plateau at high p/p_0 values and an almost vertical and parallel behavior of both isotherm branches through a vast range of values of the ordinate axis. This behavior is typical for type IV isotherms and is frequently associated with rigid and ordered spherical porous materials of uniform size.[21,22]

The empty capsules exhibit a high pore volume of 1.3 $cm^3\ g^{-1}$ and an unimodal pore size distribution (Fig. 7B), with average diameter of 14.4 nm as determined by the BJH method.[14,22] Upon encapsulation/immobilization, PHMB@silica capsules showed a noteworthy decrease in the pore volume and surface area values (see Table 1), thereby suggesting that PHMB immobilization induces significant changes on the capsule porosity. Furthermore, the pore size distribution is largely shifted to lower pore diameters with an average value of 4.4 nm. These results can be explained by taking into account the dimension and morphology of the PHMB molecule (conformation chain, hydrophobicity and charge density) which, during capsule formation occupy the pores.

3.2.5. Thermogravimetric analysis. Thermogravimetry experiments were performed in order to verify the thermal behavior of both empty and PHMB containing silica capsules, as well as for the determination of the amount of encapsulated antimicrobial agent. Thermogravimetric analysis of calcined silica capsules was performed as a reference (Fig. 8). When comparing calcined *vs.* empty silica capsules, there is *ca.* 13% of weight loss detected for empty silica capsules. This weight loss is ascribed to degradation of incompletely hydrolyzed and condensed TEOS and possibly to some residual amount of surfactants used in the synthesis.[23]

Regarding the TGA curve of PHMB (dash-point line), a weight loss at *ca.* 200–210 °C was assigned to the onset thermal decomposition of PHMB.[24] PHMB showed intensive thermal decomposition at *ca.* 240 °C, 360 °C and 520 °C. These weight losses correspond to the loss of guanidine chain ends, degradation of guanidine from broken biguanide groups and carbonization of the molecule backbone, respectively.[8] Up to 200 °C a negligible weight loss is observed and may be attributed to water molecules adsorbed onto PHMB. The curve corresponding to PHMB@silica capsules between 250 and 700 °C is different from that observed for the empty capsules, but similar to the curve obtained for PHMB alone. However, unlike to solely PHMB, the immobilization of polymer inside silica shell did not reveal a sharp thermal degradation in the range of 350–400 °C. This fact indicates a strong interaction between PHMB and silica. Similar features were observed before with cellulose–silica hybrids, where cellulosed formed hydrogen bonding to silica.[25]

The differences in weight loss observed between empty silica capsules and those filled with PHMB revealed the amount of loaded PHMB, which was *ca.* 24 wt% (Fig. 8). According to these findings, encapsulation efficiency was determined to be 20%.

3.3. Quantitative analysis of PHMB by UV-Vis spectroscopy

For quantitative analysis and release of PHMB from the capsules, calibration curves of the drug were performed in water, ethanol 70% and PBS (pH 7.0). Fig. 9 shows the UV-Vis spectra of PHMB (20% w/w) in those media, demonstrating the maximum absorbance of PHMB at $\lambda = 235$ nm in water and PBS solution and $\lambda = 236$ nm in ethanol.

The loading content obtained by release of PHMB in deionized water was *ca.* 22 wt%. The slightly higher amounts of loaded PHMB obtained by TG analysis may be due to the fact that the simple extraction with water is not able to entirely remove the polymer trapped inside the pores, leaving a small amount of the polymer inside.

The total amount of PHMB released from capsules was determined by suspending PHMB@silica capsules in different solvents, under stirring, for a 24 h period at room temperature. Different solvents (water, 70% ethanol, and PBS) were chosen due to different solubility of PHMB in these media and their relevance for biological studies. Besides, 70% ethanol was chosen due to the fact that cleansing wipes and cleansing solutions are known to have ethanol (70–90%) in their composition, being relevant for applications of PHMB encapsulated in silica capsules. PHMB release reached 88%, 68% and 63% for

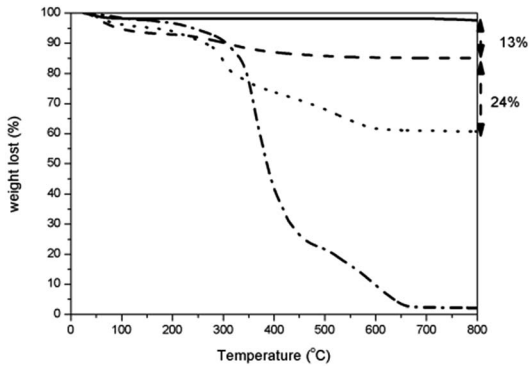

Fig. 8 TGA curves of (·) PHMB, ( ) calcined silica capsules, ( ) empty silica capsules and (···) PHMB@silica capsules.

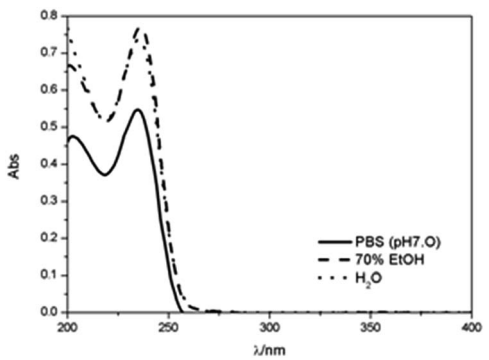

Fig. 9 UV-Vis spectra of PHMB (4.73×10^{-6} mol dm^{-3}) in (▬) PBS at pH 7.0, (▬ ▬) 70% ethanol and (●●●) water.

water, 70% ethanol and PBS pH 7.0, respectively. The reduced release of PHMB in ethanol, when compared to water, was expected since the solubility of PHMB is greater in water than in ethanol.[8] On the other hand, the lower release of PHMB in PBS solution, when compared to deionized water, can be attributed to the presence of salts in the buffer solution that cause a decrease in the polymer solubility.[26]

PHMB release studies were performed in PBS pH 7.4 (Fig. 10), to establish a correlation with antimicrobial assessment results shown in Section 3.4.

The release of PHMB from capsules in PBS pH 7.4 solution reaches *ca.* 59% of the initial loading content (determined by TG analysis) after 30 min. This fast release might be due to the fact that a fraction of PHMB is trapped at the capsule surface. After this time, the release of PHMB reaches a plateau, which remained constant (within error) for the whole period sampled.

In order to understand the release behaviour of PHMB from the silica capsules, several kinetic models were fitted to the experimental data, such as first and pseudo-first order, Higuchi, Hixon–Crowell, Ritger–Peppas and pseudo-second order. Pseudo first order and pseudo second order kinetic equations commonly are used in desorption studies.[27] From all the aforementioned models, only the pseudo-second order (eqn (2)) fitted the whole range of experimental release data, with a high correlation coefficient (R^2).[28 31]

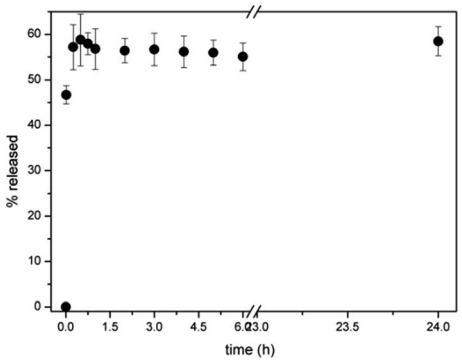

Fig. 10 Release profile of PHMB from silica capsules in PBS at pH 7.4.

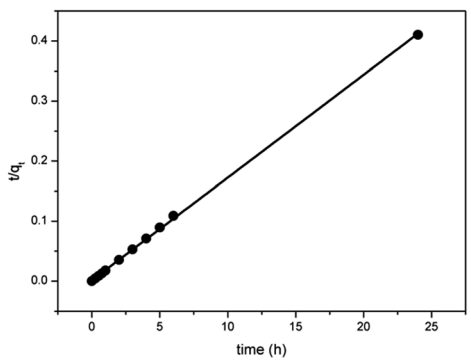

Fig. 11 Fitting of data for PHMB release silica capsules according to a pseudo-second order kinetic model.

Table 2 Drug release kinetic data obtained from pseudo-second order fitting of PHMB release from silica capsules

Sample	q_e (exp)	k (mg h ^{1})	q_e[a]	R^2
PHMB@silica capsules	58.79	0.2284	58.48	0.9997

[a] Estimated from pseudo second order kinetic model.

$$t/q_t = 1/kq_e^2 + t/q_e \quad (2)$$

where q_e and q_t are the equilibrium release amounts and the release amounts at any time (t), respectively.

Based on this model, the fitted results of PHMB release profiles are given in Fig. 11 and Table 2.

The q_e values obtained from the pseudo-second order fitting and presented in Table 2 are consistent with the experimental values obtained for q_e. This indicates that PHMB release data is consistent with a desorption process in the entire range of time sampled.

At this point, the exact location of PHMB on silica capsules can be discussed based on results obtained and complemented by different techniques. On one hand the positive zeta potential measured in the presence of PHMB is consistent with the cationic nature of this polymer and its location on the surface of silica, which somehow explains a desorption-like mechanism for the release of PHMB. However, these results do not exclude the fixation of PHMB in the inner region (pores) of silica capsules. The walls of silica porous materials are completely covered with silanol groups, allowing a large range of molecules to be confined inside the materials pore network.[32,33] Herein, this is supported by significant changes in the textural properties, namely a significant decrease in surface area and pore size upon PHMB encapsulation/immobilization. In addition, the interactions between the immobilized molecules and capsules are frequently associated with hydrogen bonding and electrostatic interactions,[34] which is in agreement with the TG results obtained for PHMB@silica capsules.

3.4. Antimicrobial activity assessment

The bactericidal effect of PHMB@silica capsules was compared with the activity of the free polymer (PHMB), potential bactericides used in the synthesis of silica capsules (surfactants), empty silica capsules, as well as the medium (PBS) used for the microbiological studies.

The results for a 240 min time span and for the reference PHMB concentrations of 20 and 200 ppm, are presented in Fig. 12 and 13, respectively. Considering that because of operational limitations, bioluminescence was not read immediately upon the addition of the tested materials and a time lapse of up to 5 min may have occurred, the initial bioluminescence in the control suspension (PBS) was plotted as a theoretical time-zero value, and initial readings in all treatments were plotted as corresponding to a 5 min exposure.

In experiments conducted with 20 ppm of PHMB, the biocidal effect expressed as a decrease in light emission by the bioluminescent bacteria in relation to the control (PBS), was higher for

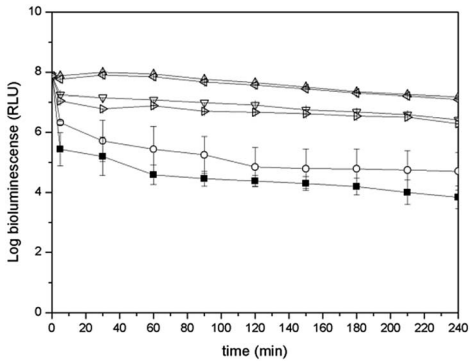

Fig. 12 Inhibition of a recombinant bioluminescent strain of *Escherichia coli* under different experimental conditions corresponding to 20 ppm of biocide: free PHMB (-■-), PHMB@silica capsules (-○-), PBS (-△-), Tween® 20 (-▽-), empty silica capsules (-◁-) and Span® 85 (-▷-).

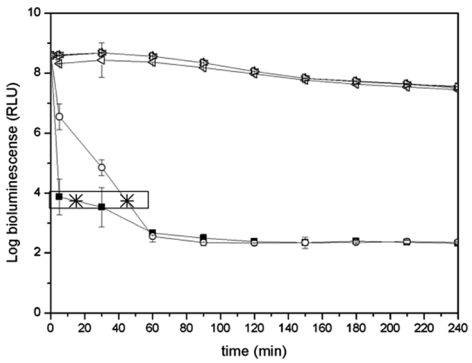

Fig. 13 Inhibition of a recombinant bioluminescent strain of *Escherichia coli* under different experimental conditions corresponding to 200 ppm of biocide: free PHMB (-■-), PHMB@silica capsules (-○-), PBS (-△-), Tween® 20 (-▽-), empty silica capsules (-◁-) and Span® 85 (-▷-).

free PHMB (3.3 log) than for PHMB@silica capsules (2.5 log). Empty capsules and surfactants had no significant bactericidal action (ANOVA, $p > 0.05$), corresponding to <1 log reduction in light emission. In the experiments with PHMB concentrations of 200 ppm, silica capsules and surfactants did not cause significant inhibition (ANOVA, $p > 0.05$), which is in accordance with what has been reported for empty silica capsules.[35] Although the antimicrobial efficiency of encapsulated PHMB was reduced in comparison to the free polymer for the first 60 min (ANOVA, $p < 0.05$), similar inactivation factors were achieved (4.2 log reduction in light emission) at the end of the experiment (ANOVA, $p > 0.05$) (Fig. 13). Considering that a maximum release of biocide from the PHMB@silica capsules was attained after 30 min and that the effect of the biocide in the free form occurs mainly during the initial 15 min of exposure, the observed delay in antimicrobial activity of PHMB@silica capsules is considered consistent with PHMB release from capsules and triggering of the biological effect (points highlighted with ✳ in Fig. 13).

The bacterial inactivation obtained with PHMB@silica capsules verifies the criterion of a minimum 3 $\log_{10}$ CFU reduction (killing efficiency of 99.9% or more) established by the American Society of Microbiology so that any new approach can be termed "antimicrobial" or "antibacterial".[36] Therefore, the observed delay in antimicrobial activity is considered consistent with PHMB release from capsules.

The promising results of PHMB on bacterial inactivation, accompanied by the possibility to immobilize it on insoluble inert silica capsules suggest that this approach can be applied in the environment. The use of immobilized PHMB allows its recovery and reuse, preventing direct interaction with any component of the ecosystem, as well as its diffusion or accumulation in the environment. Besides, the possibility to reuse the immobilized PHMB makes this approach less expensive.

4. Conclusions

Antibacterial agent polyhexamethylene biguanide (PHMB) was successfully encapsulated into silica capsules and obtained capsules were thoroughly characterized. The amount of PHMB loaded inside the capsules was determined to be 24% wt with an encapsulation efficiency of 20%. Although empty silica capsules and those filled with PHMB (PHMB@silica capsules) are both spherically shaped, the size distribution of the latter is broader. The synthesized empty silica capsules are mesoporous materials but when PHMB is encapsulated (PHMB@silica capsules) the surface area decreases significantly and there is also a decrease in pore size and volume.

Almost all PHMB encapsulated in PHMB@silica capsules (22 wt% out of the 24 wt% obtained by TGA) is leachable after 24 h stirring in water. Furthermore, the study on release of PHMB for 24 h showed that silica capsules liberate higher amounts of PHMB in water than in ethanol solution or PBS at pH 7.0.

Although an initial rapid release is observed, equilibrium was established and maintained as time progressed. The release kinetics study reveals that the drug follows pseudo-second order kinetics and the mechanism of drug release was desorption type. In PBS at pH 7.4, *ca.* 59% of PHMB is released from capsules in 24 h, most of which was leached during the first 30 min. The fact that PHMB is released from capsules over time may explain the delayed bactericidal activity of PHMB silica capsules in the presence of microorganisms.

Hence, the encapsulated PHMB in silica capsules can be used in delivery systems that require a controlled release of bactericide for a relatively short time span. In spite of the encapsulation of the bactericidal polymer causing a decrease in the kinetics of inactivation due to the delay in it liberation from capsules, similar factors of inactivation were achieved at the end of time-course experiments as with equivalent amount of free PHMB using a recombinant bioluminescent *Escherichia coli* strain as a biological model.

Acknowledgements

This work was developed in the scope of the project CICECO-Aveiro Institute of Materials (Ref. FCT UID/CTM/50011/2013), financed by national funds through the FCT/MEC and when applicable co-financed by FEDER under the PT2020 Partnership Agreement. This work is also funded by ERDF Funds through

Operational Competitiveness Programme – COMPETE in the frame of the project RENOVA PAPTIS – FCOMP-01-0124-FEDER-30203 and Centre for Environmental and Marine Studies (CESAM) unit project Pest-C/MAR/LA0017/2013. FM thanks FCT for PhD grant SFRH/BD/72663/2010 and JT thanks FCT for researcher grant IF/00347/2013. The authors would like to thank Doctor Sónia Patrício for the helpful insights on surface area and pore volume results.

References

1 K. S. Rao, K. El-Hami, T. Kodaki, K. Matsushige and K. Makino, *J. Colloid Interface Sci.*, 2005, **289**, 125–131.
2 I. Makarovsky, Y. Boguslavsky, M. Alesker, J. Lellouche, E. Banin and J.-P. Lellouche, *Adv. Funct. Mater.*, 2011, **21**, 4295–4304.
3 A. M. Klibanov, *J. Mater. Chem.*, 2007, **17**, 2479–2482.
4 A. M. Larson and A. M. Klibanov, *Annu. Rev. Chem. Biomol. Eng.*, 2013, **4**, 171–186.
5 T. Szabó, L. Románszki and M. Pávai, *Handbook of Smart Coatings for Materials Protection*, Elsevier, 2014.
6 J.-X. Wang, Z.-H. Wang, J.-F. Chen and J. Yun, *Mater. Res. Bull.*, 2008, **43**, 3374–3381.
7 M. Küsters, S. Beyer, S. Kutscher, H. Schlesinger and M. Gerhartz, *J. Pharm. Anal.*, 2013, **3**, 408–414.
8 G. F. de Paula, G. I. Netto and L. H. C. Mattoso, *Polymers*, 2011, **3**, 928–941.
9 Arch Chemicals, *Vantocil® IB Technical Information Bulletin*, 2008.
10 A. D. Lucas, E. A. Gordon and M. E. Stratmeyer, *Talanta*, 2009, **80**, 1016–1019.
11 T. Ristić, L. Fras, M. Novak, M. Kralj Kunčič, S. Sonjak, N. Gunde-Cimerman and S. Strnad, *Science Against Microbial Pathogens: Communicating Current Research and Technological Advances*, Formatex Research Center, 2011, vol. 3, pp. 36–51.
12 T. Rowhani and A. F. Lagalante, *Talanta*, 2007, **71**, 964–970.
13 S. Ashraf, N. Akhtar, M. A. Ghauri, M. I. Rajoka, Z. M. Khalid and I. Hussain, *Nanoscale Res. Lett.*, 2012, **7**, 267–273.
14 K. S. W. Sing, D. H. Everett, R. A. W. Haul, L. Moscou, R. A. Pierotti, J. Rouquerol and T. Siemieniewska, *Pure Appl. Chem.*, 1985, **57**, 603–619.
15 E. Alves, C. B. Carvalho, J. C. Tomé, M. F. Faustino, M. P. M. S. Neves, A. Tomé, J. S. Cavaleiro, Â. Cunha, S. Mendo and A. Almeida, *J. Ind. Microbiol. Biotechnol.*, 2008, **35**, 1447–1454.
16 W. Paulus, *Directory of Microbicides for the Protection of Materials-A Handbook*, Springer, Netherlands, 2005.
17 L. Zhang, M. D'Acunzi, M. Kappl, G. K. Auernhammer, D. Vollmer, C. M. van Kats and A. van Blaaderen, *Langmuir*, 2009, **25**, 2711–2717.
18 J. Casas-Sanchez, M. K. Herrlein, D. I. Collias, M. D. Mitchell and T. J. Wehmeier, *US Pat.* US20080287019A1, 2008.
19 J.-F. Chen, H.-M. Ding, J.-X. Wang and L. Shao, *Biomaterials*, 2004, **25**, 723–727.
20 F. Rouquerol, J. Rouquerol and K. Sing, in *Adsorption by Powders and Porous Solids*, ed. F. Rouquerol, J. Rouquerol and K. Sing, Academic Press, London, 1999.
21 K. Sing and R. Williams, *Adsorpt. Sci. Technol.*, 2004, **22**, 773–782.
22 K. S. W. Sing, *Adv. Colloid Interface Sci.*, 1998, **76–77**, 3–11.
23 F. Maia, J. Tedim, A. D. Lisenkov, A. N. Salak, M. L. Zheludkevich and M. G. S. Ferreira, *Nanoscale*, 2012, **4**, 1287–1298.
24 ECHA, *Annex 1: Background document to the Opinion proposing harmonised classification and labelling at Community level of Polyhexamethylene biguanide*, 2011.
25 S. Sequeira, D. V. Evtuguin and M. I. Portugal, *Polym. Compos.*, 2009, **30**, 1275–1282.
26 W. G. Bauer, T. J. Balzar, S. L. Christoffel, A. M. Przepasniak and M. E. Sojka, *US Pat.* US20070147942A1, 2010.
27 H. Bashiri, *Phys. Chem.*, 2012, **2**, 80–85.
28 B. AppaRao, M. R. Shivalingam, Y. V. Kishore Reddy, N. Sunitha, T. Jyothibasu and T. Shyam, *Int. J. Pharm. Biomed. Res.*, 2010, **1**, 90–93.
29 G. Maria and I. Luta, *Chem. Pap.*, 2011, **65**, 542–552.
30 S. H. Hussein-Al-Ali, M. E. E. Zowalaty, M. Z. Hussein, M. Ismail and T. J. Webster, *Int. J. Nanomed.*, 2014, **9**, 549–557.
31 Y. S. Ho and G. McKay, *Process Biochem.*, 1999, **34**, 451–465.
32 M. Vallet-Regí, *J. Intern. Med.*, 2010, **267**, 22–43.
33 D. Das, Y. Yang, J. S. O'Brien, D. Breznan, S. Nimesh, S. Bernatchez, M. Hill, A. Sayari, R. Vincent and P. Kumarathasan, *J. Nanomater.*, 2014, **2014**, 176015, 12pages.
34 Z. Li, J. C. Barnes, A. Bosoy, J. F. Stoddartbc and J. I. Zink, *Chem. Soc. Rev.*, 2012, **41**, 2590–2605.
35 F. Maia, A. P. Silva, S. Fernandes, A. Cunha, A. Almeida, J. Tedim, M. L. Zheludkevich and M. G. S. Ferreira, *Chem. Eng. J.*, 2015, **270**, 150–157.
36 ASM (2015), Antimicrobial Agents and Chemotherapy, Instructions to authors, 1, 73–76.